Journal of Southeast University (English Edition) Vol. 42, No. 1, pp. 92-99 Mar. 2026 ISSN 1003-7985

Constitutive damage model for polypropylene fiber-reinforced recycled fine aggregate concrete under compressive loading

LUO Bin, CAO Guang, SONG Yechao, ZHAO Fengnian, TANG Zhonghua

(School of Civil and Hydraulic Engineering, Lanzhou University of Technology, Lan Zhou 730050, China)

Abstract: To promote the application of green recycled construction materials in civil engineering, this study presents a statistical damage constitutive model for polypropylene fiber recycled fine aggregate concrete (PRFAC), based on the strain equivalence principle and the assumption that microelement strength follows a Weibull statistical distribution. The proposed model incorporates the Drucker-Prager failure criterion. By examining the influence of Weibull distribution parameters m and S_0 on the stress-strain response, empirical relationships were established between the fine aggregate replacement ratio and the distribution parameters. This enabled the derivation of a theoretical stress-strain curve accounting for variable recycled fine aggragate (RFA) replacement ratios. The experimental results show that the proposed model exhibits high agreement with measured data and effectively captures the increased brittleness of PRFAC with higher RFA replacement ratios. Moreover, increasing the replacement rate accelerates internal crack propagation, reduces deformability and toughness, and significantly hastens the accumulation of internal damage in PRFAC.

Key words: green concrete; polypropylene fibers; recycled fine aggregate; damage constitutive model; compressive behavior; aggregate replacement ratio

DOI: 10. 3969/j. issn. 1003-7985. 2026. 01. 009

With the rapid advancement of urban construction in China, a significant number of old buildings have been demolished, resulting in construction and demolition waste, of which more than 30% comprises waste concrete [1]. Utilizing such waste materials as aggregate in concrete production yields recycled concrete, which facilitates the reuse of discarded concrete and contributes to the broader goal of sustainable development [2-3]. However, the mechanical and durability properties of recycled concrete are generally inferior to those of conventional concrete, limiting its widespread application in engineering practice [4].

Polypropylene fibers—characterized by low self-weight, corrosion resistance, crack-bridging ability, and toughness enhancement—have demonstrated the potential to improve the mechanical behavior of recycled concrete[5-6]. For example, Das et al. [7] experimentally confirmed that the inclusion of polypropylene fibers significantly increases both the splitting tensile strength and flexural strength of recycled concrete. Using scanning electron microscopy, He et al. [8] observed that incorporating fibers into recycled aggregate concrete improves the compactness and homogeneity of the cement matrix, while also refining the microstructure of the interfacial transition zones between aggregate/paste and fiber/paste. Similarly, Ahmed et al. [9] reported that the inclusion of polypropylene fibers substantially enhances the compressive strength of recycled concrete at various recycled fine aggregate (RFA) replacement ratios.

In recent years, prefabricated concrete structures have gained increasing adoption due to their advantages in standardized design, factory-based production, and modularized on-site assembly. The release of national standards, such as Technical Specification for Prefabricated Concrete Structures (JGJ 1—2014) and Technical Standard for Prefabricated Concrete Buildings (GB/T 51231—2016), has further highlighted the pivotal role of prefabricated concrete in transforming and upgrading the traditional construction industry[10-11]. Incorporating recycled concrete into the production of precast components for prefabricated structures would not only promote substantial resource conservation but also represent an important pathway toward achieving the dual-carbon goals within the construction sector[12-14].

To this end, we previously developed a polypropylene fiber RFA concrete (PRFAC) through an optimized mix design with the goal of applying it in precast components for prefabricated concrete structures. To enable the numerical simulation and analysis of PRFAC, this study—building upon earlier research on material development—establishes a statistical damage constitutive model for fiber-reinforced RFA concrete. The model is developed based on the strain equivalence principle, assuming that the microelement strength of PRFAC follows a Weibull statistical distribution, which effectively captures the heterogeneity and probabilistic nature of damage evolution

Received 2025-07-10, **Revised** 2025-09-29.

Biography: LUO Bin (1985—), male, doctor, associate professor, luobin@lut. edu. cn.

Foundation item: The National Natural Science Foundation of China (No. 52168022).

Citation: LUO Bin, CAO Guang, SONG Yechao, et al. Constitutive damage model for polypropylene fiber-reinforced recycled fine aggregate concrete under compressive loading[J]. Journal of Southeast University (English Edition), 2026, 42(1): 92-99. DOI: 10. 3969/j. issn. 1003-7985. 2026. 01. 009.

in recycled concrete[15-16]. Furthermore, it is assumed that microelement failure conforms to the Drucker-Prager (D-P) criterion, which more accurately represents the yield behavior of concrete-like materials under the influence of hydrostatic pressure[17-18], thereby better reflecting the plastic deformation capacity of the material under complex stress states.

Furthermore, by analyzing the effects of the distribution parameters m and S_0 on the model's stress-strain response, empirical relationships between the RFA replacement ratio and these distribution parameters were derived. This enabled the establishment of theoretical statistical damage stress-strain curves for PRFAC, incorporating the RFA replacement ratio as a variable parameter.

1 Experiment

1.1 Materials

The primary materials used in this study included cement, coarse aggregate, fine aggregate, polypropylene fibers, water, and a superplasticizer (to enhance the workability of RFA). The cement was 42.5-grade Ordinary Portland Cement produced by Anhui Conch Cement Co., Ltd. The coarse aggregate was a continuously graded crushed stone with particle sizes ranging from 5 to 25 mm. The fine aggregate was a mixture of natural river sand and RFA. Their physical and mechanical properties are presented in Table 1. The polypropylene fibers used were monofilament-type, with an equivalent diameter of 18-45 μm, a tensile strength of 400 MPa, an elongation at break of 5%-20%, an elastic modulus of 3.5 GPa, and a specific gravity of 0.91 g/cm^3.

Table 1 Comparison of properties between natural sand and recycled fine aggregate

Aggregate type	Bulk density/ (kg·m^{-3})	Apparent density/ (kg·m^{-3})	Crushing index/%	Water absorption/ %	Fineness modulus
Natural sand	1 544	2 657	14	0.8	2.8
Recycled fine aggregate	1 342	2 419	29	8.0	3.0

1.2 Specimen preparation and loading procedure

Since this study focuses on examining the influence of the fine aggregate replacement ratio on the compressive damage constitutive model of PRFAC, the mix proportions for 1 m^3 of PRFAC used in this experiment were determined based on our previous findings: 400 kg of cement, 180 kg of water, 1 165 kg of natural coarse aggregate, 1.5 kg of polypropylene fibers, and 6.0 kg of superplasticizer. The RFA replacement ratio (denoted as η) was varied across 11 levels: 0%, 10%, 20%, 30%, 40%, 50%, 60%, 70%, 80%, 90%, and 100%, and the corresponding specimen groups were labeled TB1-TB11.

To ensure experimental consistency, six specimens were prepared for each mix design using prismatic concrete samples with dimensions of 150 mm × 150 mm × 300 mm. A dry mixing method was used, in which the polypropylene fibers, sand, coarse aggregate, and cement were initially mixed uniformly, followed by the addition of water and continued mixing.

After 28 d of curing under standard conditions, all specimens were subjected to uniaxial compression using a servo-controlled rigid testing machine at constant strain rate loading. The loading rate was maintained at 0.05 mm/min[19]. To simultaneously measure the elastic modulus, longitudinal strain gauges were affixed to two opposing faces along the central vertical axis of each specimen, and a vertical displacement transducer was placed on the side surface to compare with the strain gauge readings, as shown in Fig. 1.

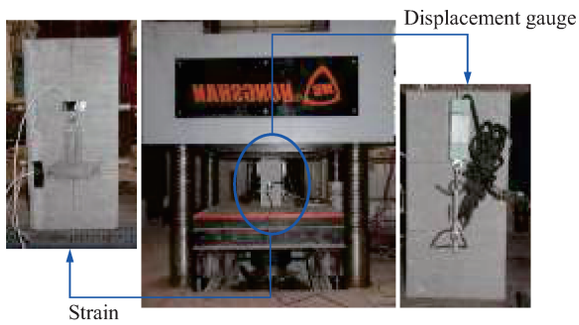

Fig. 1 Test setup

1.3 Results and analysis

The initial vertical cracks first appeared at the corners for all specimens (TB1-TB11). As the load increased, these cracks propagated and widened along the loading direction toward the specimen center. Near failure, through-cracks developed on the surface, and local crushing occurred at some corners. The presence of polypropylene fibers partially inhibited the rapid development of cracks, thereby preventing large-scale spalling. The specimens exhibited plastic failure modes and retained their overall structural integrity. The final failure morphology resembled a "lantern" shape, with cracks distributed in a hyperbolic pattern along the specimen sides and slight outward bulging at the corners in some cases (Fig. 2) using TB1 and TB11 as examples.

The stress-strain curves shown in Fig. 3 reveal that specimens TB2-TB11 followed a mechanical response similar to that of TB1, undergoing distinct stages: elastic, elastoplastic, peak, descending, inflection point, and residual segments, where σ denotes the nominal stress, ε denotes the strain, f_c is the compressive strength corresponding to peak load, ε_p is the peak strain. Before reaching the peak stress, the ascending portions of the curves across different RFA replacement ratios (η) exhibited minimal variation and nearly overlapped. In contrast, the descending branch beyond the peak point be-

(a) (b)

Fig. 2 Axial compressive failure modes of PRFAC prism specimens. (a) TB1; (b) TB11

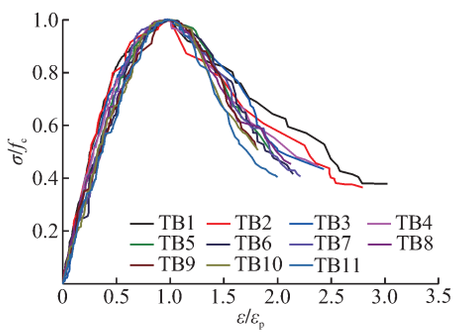

Fig. 3 Dimensionless stress-strain curves of PRFAC under axial compression

comes progressively steeper with increasing η. This trend is primarily attributed to the presence of microcracks within the RFA and numerous impurities, which adversely affect the cement hydration degree and weaken the interfacial bonding between different phases in the concrete. These results show that the ductility and deformability of PRFAC decrease as the replacement ratio η increases.

The key characteristic points extracted from the stress-strain curves of TB1-TB11 are summarized in Table 2. With the exception of TB6, the compressive strength f_c of the other 10 specimens was lower than that of TB1. Apart from TB2, the peak strain ε_p of specimens TB3-TB11 generally exhibited an increasing trend with the rise in the replacement ratio η. The elastic modulus E of specimens TB2-TB11 was consistently lower than that of TB1, and E decreased progressively as η increased.

This trend is attributed to the inherent microcracks and lower strength of RFAs compared to river sand. As η increased, the porosity of the cementitious matrix also increased, reducing f_c and E values, and increasing ε_p. Regarding the observation that the f_c of specimen TB6 is approximately 1% higher than that of TB1, this study attributes this phenomenon primarily to the limited sample size, which may have introduced a degree of data scatter into the experimental results.

Table 2 Characteristic point results of PRFAC under uniaxial compression

Specimen	P/kN	f_c/MPa	$\sigma_{0.2}$/MPa	$\varepsilon_p/10^{-3}$	$\varepsilon_{0.85}/10^{-3}$	E/GPa
TB1	845.89	37.60	7.52	2.91	3.82	25.09
TB2	825.10	36.67	7.33	2.80	3.60	24.96
TB3	815.52	36.25	7.25	2.95	4.13	21.44
TB4	746.88	33.19	6.64	3.13	4.14	20.24
TB5	789.50	35.09	7.02	3.28	4.57	18.45
TB6	872.22	38.77	7.75	3.47	4.85	18.11
TB7	834.75	37.10	7.42	3.57	4.77	15.02
TB8	726.77	32.30	6.46	3.38	4.44	16.48
TB9	748.57	33.27	6.65	3.59	4.97	13.61
TB10	762.73	33.89	6.78	3.62	4.72	13.98
TB11	688.50	30.60	6.12	3.85	4.81	10.30

Note: P denotes the peak load; $\sigma_{0.2}$ represents the residual stress at 0.2% strain; $\varepsilon_{0.85}$ is the strain corresponding to 85% of f_c.

2 Statistical Damage Constitutive Model

2.1 Development of the damage constitutive model

According to the strain equivalence hypothesis proposed by Jean[20], the damage constitutive relationship of PRFAC can be expressed as follows:

$$\tilde{\sigma} = \frac{\sigma}{1-D} = \frac{E\varepsilon}{1-D} \tag{1}$$

$$D = \frac{A^{\mathrm{D}}}{A} \tag{2}$$

$$A = \tilde{A} + A^{\mathrm{D}} \tag{3}$$

where $\tilde{\sigma}$ denotes the effective stress; D denotes the damage variable; $\tilde{A}$ denotes the load-bearing area of the undamaged portion; A^{D} denotes the area of the damaged portion.

Assuming that the macroscopic PRFAC model is composed of an infinite number of microelements, and that each microelement obeys generalized Hooke's law prior to failure and follows a Weibull statistical distribution[21], the probability density function of the strength of microelements can be expressed as follows:

$$P(S) = \frac{m}{S_0}\left(\frac{S}{S_0}\right)^{m-1}\exp\left[-\left(\frac{S}{S_0}\right)^{m}\right] \tag{4}$$

where m denotes the shape parameter; and S_0 denotes the scale parameter. Both parameters are nonnegative and intrinsic to the Weibull distribution.

Let D be the ratio of the number of failed microelements N_d to the total number of microelements N under a given level of applied stress, which gives

$$D = N_d/N \tag{5}$$

$$N_d = \int_0^S NP(S)\,\mathrm{d}F = N\left\{1-\exp\left[-\left(\frac{S}{S_0}\right)^{m}\right]\right\} \tag{6}$$

Substituting Eq. (6) into Eq. (5) yields the final ex-

pression for the statistical damage variable as

$$D = 1 - \exp\left[-\left(\frac{S}{S_0}\right)^m \right] \tag{7}$$

By substituting Eq. (7) into Eq. (1), the statistical damage constitutive relationship of PRFAC under triaxial compression is obtained, as expressed in Eq. (8):

$$\nu\sigma_i = E\varepsilon_i \exp\left[-\left(\frac{S}{S_0}\right)^m \right] + \nu(\sigma_j + \sigma_k) \tag{8}$$

where ν denotes Poisson's ratio; and i, j, $k = 1, 2, 3$ denote the tensor indices in Cartesian coordinates.

According to the research and summarization of concrete failure criteria by Guo [22], and to simplify the formulation, we adopted the Drucker-Prager failure criterion to represent the microelement strength S of PRFAC, as follows:

$$S = \alpha I_1 + \sqrt{J_2} \tag{9}$$

where $\alpha = \sin\varphi / \sqrt{9 + \sin^2\varphi}$, φ denotes the internal friction angle of the concrete material, typically taken as an approximate value of 35.6° [23]; I_1 and J_2 are the first stress and second deviatoric stress invariants, respectively. The expressions for I_1 and J_2 are obtained according to Ref. [24], i.e., Eqs. (10) and (11).

$$I_1 = \frac{(\sigma_1 + 2\sigma_3)E_0\varepsilon_1}{\sigma_1 - 2\nu\sigma_3} \tag{10}$$

$$\sqrt{J_2} = \frac{(\sigma_1 - \sigma_3)E_0\varepsilon_1}{\sqrt{3}\,(\sigma_1 - 2\nu\sigma_3)} \tag{11}$$

where σ_1 and σ_3 denote the nominal stress measurable in the triaxial test.

2.2 Distribution parameters

As shown in Eq. (8), the proposed model involves only two undetermined parameters: m and S_0. If these two parameters can be related to macroscopic mechanical properties of concrete and expressed accordingly, the model would not only reflect clearer physical interpretations but also offer a more generalized and practical method for parameter identification.

Thus, according to the methodology in Ref. [25], this study employs characteristic points from the stress-strain curve of PRFAC to derive specific expressions for the distribution parameters. The derivation is based on the following boundary conditions:

Boundary conditions are as follows: (1) $\varepsilon = \varepsilon_p$, $\sigma = \sigma_p$; (2) $\left.\frac{d\sigma}{d\varepsilon}\right|_{\varepsilon=\varepsilon_p} = 0$; where σ_p denotes the peak stress. Under triaxial compression with equal confining pressures, substituting Eq. (9) into Eq. (8) yields the statistical damage constitutive model of PRFAC as follows:

$$\exp\left(\frac{S_p}{S_0}\right)^m = \frac{E_0\varepsilon_p}{\sigma_p - 2\nu\sigma_3} \tag{12}$$

$$m = \frac{1}{\ln\left[E_0\varepsilon_p/(\sigma_p - 2\nu\sigma_3)\right]} \tag{13}$$

From Eqs. (12) and (13), the distribution parameters m and S_0 can be obtained using the boundary conditions. Together with the previously defined mechanical variables, this yields a complete stochastic damage constitutive model of PRFAC.

For the uniaxial compression, where $\sigma_2 = \sigma_3 = 0$, the statistical damage constitutive relationship and the corresponding parameter expressions are simplified as follows:

$$\begin{cases} \sigma = E\varepsilon \exp\left[-\left(\dfrac{S}{S_0}\right)^m\right] \\ m = \dfrac{1}{\ln(E\varepsilon_p/\sigma_p)} \\ \left|\dfrac{S_p}{S_0}\right|^m = \dfrac{1}{m} \end{cases} \tag{14}$$

2.3 Influence of m, S_0, and η

As previously discussed, the parameters m and S_0 have a significant influence on the statistical damage constitutive model of PRFAC. These parameters essentially control the geometrical shape and curvature of the material's stress-strain response. Table 3 presents the computed values of m and S_0 for specimens TB1-TB11 based on Eq. (14). To illustrate their respective effects on the damage model, the case of TB4 is selected as a representative example.

As presented in Table 3, the parameters for TB4 are $m = 1.398$ and $S_0 = 65.682$. By varying either m or S_0 while keeping all other variables constant, the resulting statistical damage stress-strain curves for TB4 are shown in Fig. 4. The following observations can be made:

(1) Effect of m. The shape parameter m has a negligible influence on the ascending portion of the curve. However, as stress approaches its peak value, the curve becomes increasingly sensitive to changes in m. Specifically, higher values of m result in increased peak stress and a steeper postpeak slope, indicating greater material brittleness. Therefore, m can be interpreted as an indicator of both the dispersion in the microelement strength distribution and the brittleness of PRFAC.

(2) Effect of S_0. The scale parameter S_0 also has a minimal effect in the early loading stage. As stress increases beyond a certain level, the curve begins to diverge based on different S_0 values. Larger S_0 values correspond to higher peak stresses, indicating that S_0 reflects the macrolevel average statistical strength of PRFAC. Since the stress-strain curves postpeak tend to align almost parallel, changes in S_0 do not significantly influence the softening modulus.

Table 3 Distribution parameters under different RFA replacement ratios

Specimen	η/%	Distribution parameters	
		m	S_0
TB1	0	1.153	77.091
TB2	10	1.208	74.756
TB3	20	1.427	71.253
TB4	30	1.398	65.682
TB5	40	1.645	66.418
TB6	50	2.286	65.678
TB7	60	1.741	68.978
TB8	70	1.959	57.741
TB9	80	2.185	57.293
TB10	90	2.289	57.190
TB11	100	3.237	45.608

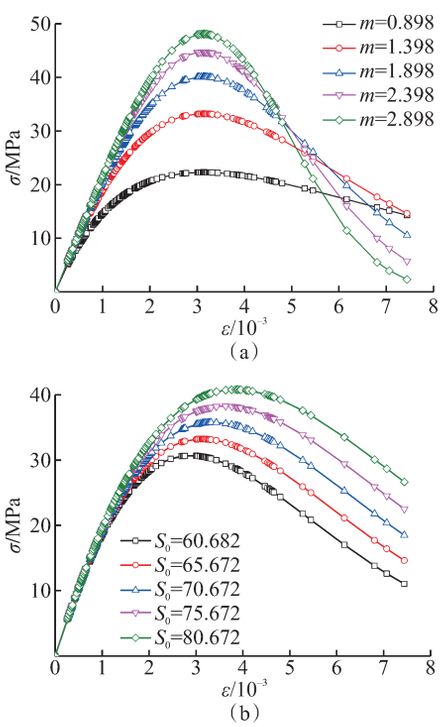

Fig. 4 Statistical stress-strain curves of TB4 under different m and S_0. (a) Different m values; (b) Different S_0 values

Table 3 reveals that the value of m generally increases with increasing RFA replacement ratio η. The m shapes the stress-strain response, suggesting that higher RFA content leads to greater dispersion in the microelement strength, thereby reducing ductility and increasing brittleness in PRFAC. Additionally, S_0 gradually decreases with increasing RFA replacement ratio η, i. e., the macrolevel average strength of PRFAC decreases with increasing RFA. Therefore, the peak stress of PRFAC gradually decreases with increasing RFA.

To better characterize the influence of the RFA replacement ratio on the damage behavior of PRFAC, and based on the observed correlation trends between the parameters m, S_0, and the RFA replacement ratio η, the relationship between m and η was fitted using a nonlinear exponential function (Eq. (15)), whereas the relationship between S_0 and η was fitted using a quadratic polynomial function (Eq. (16)).

$$m(\eta) = A_1 e^{A_2\eta} + A_3 \tag{15}$$

$$S_0(\eta) = A_4\eta^2 + A_5\eta + A_6 \tag{16}$$

where A_1-A_6 represent the fitting coefficients. By applying the values of m and S_0 for specimens TB1-TB11 from Table 3 to Eqs. (15) and (16), the coefficients A_1-A_6 can be determined, resulting in Eqs. (17) and (18). The coefficients of determination (R^2) calculated from the above equations are 0.92 and 0.87, respectively, indicating an excellent fit (Fig. 5).

$$m = 0.25e^{2.05\eta} + 1 \tag{17}$$

$$S_0 = 75.23 - 13.08\eta^2 - 12.63\eta \tag{18}$$

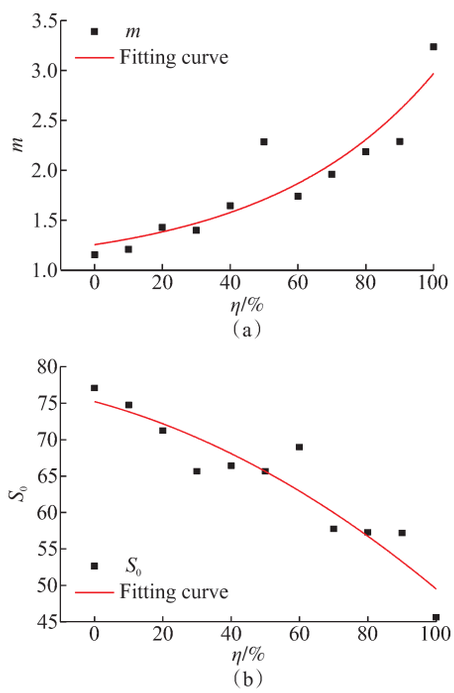

Fig. 5 Regression curves of m and S_0 with respect to η. (a) Fitting of m; (b) Fitting of S_0

2.4 Model validation

Based on the above analysis, substituting Eqs. (17) and (18) into Eq. (14) yields the statistical damage stress-strain curves of PRFAC under different η. Fig. 6 compares the theoretical curves with the experimental curves of specimens TB1-TB11.

The experimental and damage constitutive curves are consistent in the ascending branch, effectively capturing the linear elastic characteristics of this stage (Fig. 6). However, certain discrepancies were observed in the descending branch. These deviations can be attributed to the following factors: first, RFA inherently contains numerous microcracks, which influence the postpeak soft-

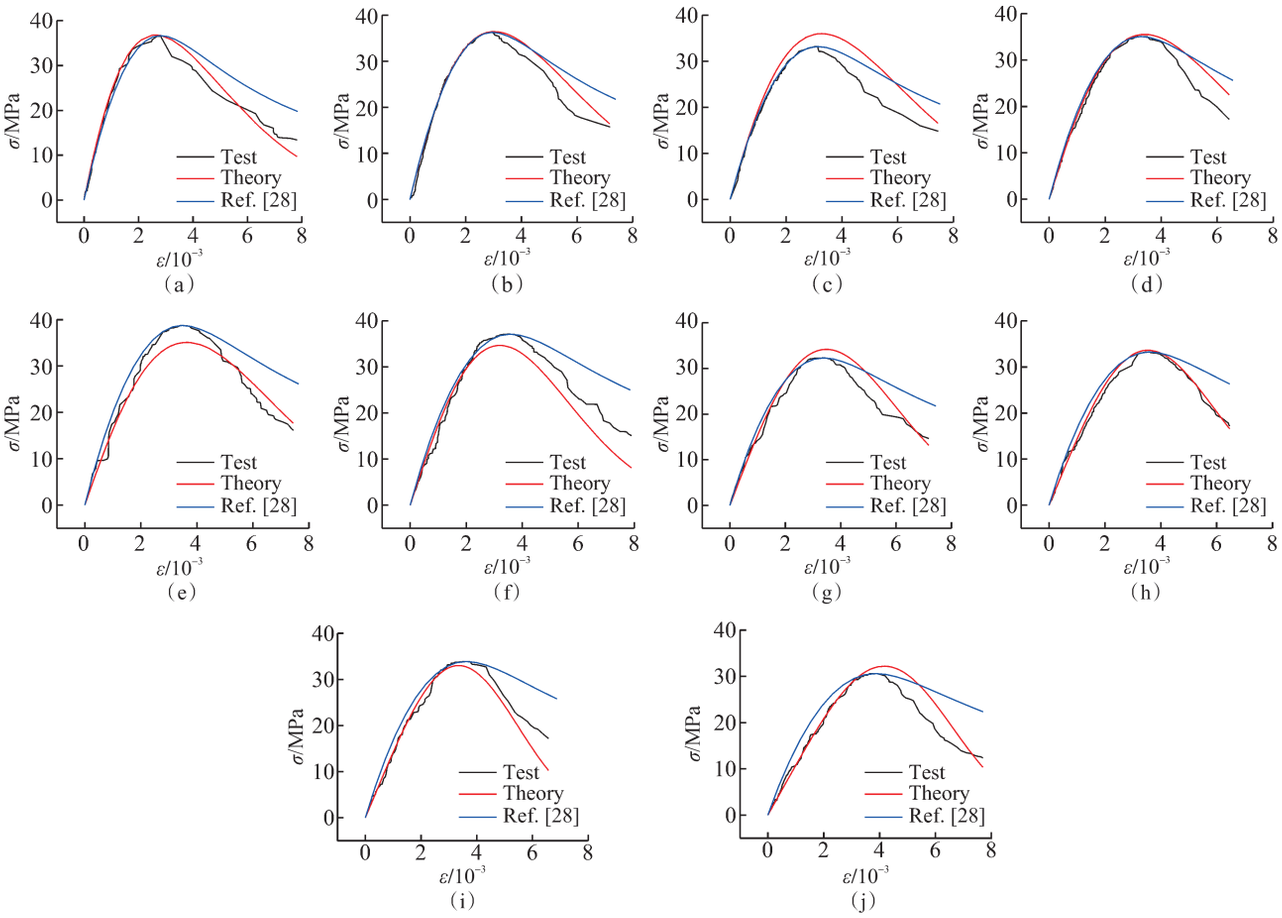

Fig. 6 Comparison between theoretical and experimental damage constitutive curves. (a) TB2; (b) TB3; (c) TB4; (d) TB5; (e) TB6; (f) TB7; (g) TB8; (h) TB9; (i) TB10; (j) TB11

ening behavior. Second, as indicated by previous studies[26-27], the incorporation of polypropylene fibers primarily enhances the flexural and splitting tensile properties of recycled aggregate concrete, with no significant effect on its compressive strength.

The proposed damage constitutive model is primarily intended for the numerical simulation of precast components in prefabricated concrete structures. To simplify the constitutive model setup in the numerical analysis, the specific influence of polypropylene fiber content on the compressive strength of PRFAC was not explicitly considered. The mechanical behavior during the fiber pull-out process in the descending branch, such as the bond stress-slip constitutive relationship, is highly complex. Collectively, these factors contribute to the observed deviations in the descending branch of the curves.

Fig. 6 demonstrates that as η increases, the descending branch of the curve becomes progressively steeper, indicating that the incorporation of RFA reduces the ductility of the concrete. Fig. 6 also includes curves derived using the uniaxial compressive constitutive equation from Ref. [28]—a commonly adopted constitutive relationship in numerical analyses of prefabricated concrete components. It is evident that the proposed damage constitutive model shows better agreement with the experimental data than the constitutive curve from Ref. [28].

In summary, the damage constitutive model established in this study effectively captures the stress-strain relationship of PRFAC under varying RFA replacement ratios. It also provides a valuable reference for defining constitutive models in the numerical analysis of prefabricated components manufactured from this sustainable material.

3 Cumulative Damage Evolution Process

Material damage is accompanied by internal energy dissipation and irreversible changes in the microstructural organization of the material. To investigate the damage mechanics behavior of PRFAC, the statistical damage variable D defined in Eq. (7) is used to calculate the cumulative damage evolution. Fig. 7 shows the relationship between the cumulative damage development rate and strain under different η values.

As shown in Fig. 7, the damage variable D remains zero at small strain levels, indicating that PRFAC is in the purely elastic phase, where the stress-strain response is linear, and no microdamage occurs. As strain increases, the damage evolution curve increases monotonically with an inverted Z-shaped pattern, indicating that

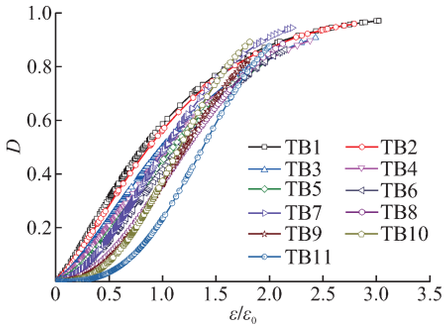

Fig. 7 Evolution of cumulative damage for PRFAC

damage accumulates continuously with growing strain as microcracks initiate and propagate within the material. The slope of the damage evolution curve gradually increases with increasing strain, indicating that the rate of damage accumulation accelerates. When the strain reaches a critical threshold, an inflection point corresponding to the peak damage rate is observed on the curve. Beyond this point, the damage accumulation slows down and eventually stabilizes until the final failure occurs.

The figure also reveals that in the initial ascending segment, specimen TB1 (0% RFA) shows a higher damage variable D than PRFAC specimens containing RFA. Additionally, higher η values are associated with lower initial D values. This phenomenon is attributed to the fact that the compaction of the cementitious matrix and closure of pre-existing microcracks in PRFAC tend to delay the onset of cumulative internal damage during early-stage compression. However, in the nonlinear loading phase, the damage evolves much more rapidly in PRFAC with higher η values. This can be explained by the inherent brittleness of RFAs compared to natural sand. The addition of RFA promotes earlier crack initiation and propagation, weakens the deformation capacity and toughness of the concrete, and ultimately accelerates the cumulative damage evolution process within PRFAC.

4 Conclusions

(1) The proposed method for deriving the distribution parameters m and S_0 is straightforward, physically meaningful, and suitable for engineering applications. The shape parameter m primarily reflects the degree of dispersion in the microelement strength distribution and the brittleness characteristics of PRFAC. The scale parameter S_0 characterizes the macrolevel average statistical strength of the material.

(2) Based on the influence of parameters m and S_0 on the stress-strain response, empirical relationships between the η and distribution parameters were established. The statistical damage constitutive curves calculated using these expressions exhibited good agreement with experimental data. The proposed model effectively captured the trend of increasing brittleness in PRFAC with higher RFA content, demonstrating its reliability and applicability for simulating PRFAC behavior under uniaxial compression.

(3) The cumulative damage evolution characteristics of PRFAC with different η values were investigated. The results show that increasing RFA content accelerates crack initiation and propagation, reduces deformability and toughness, thereby leading to a faster cumulative damage process within the material.

References

[1] GUERRERO L A, MAAS G, HOGLAND W. Solid waste management challenges for cities in developing countries[J]. Waste Management, 2013, 33(1): 220-232.

[2] LI L, XIAO J Z, HUANG K W. Numerical simulation on strain-rate sensitivity of mechanical properties of recycled aggregate concrete[J]. Journal of Southeast University (Natural Science Edition), 2017, 47(4): 776-784. (in Chinese)

[3] NEDELJKOVIĆ M, VISSER J, ŠAVIJA B, et al. Use of fine recycled concrete aggregates in concrete: A critical review[J]. Journal of Building Engineering, 2021, 38: 102196.

[4] XIAO J Z, LI W G, SUN Z H, et al. Properties of interfacial transition zones in recycled aggregate concrete tested by nanoindentation [J]. Cement and Concrete Composites, 2013, 37: 276-292.

[5] HUANG W, QUAN W L, GE P. Orthogonal tests investigation into hybrid fiber-reinforce recycled aggregate concrete and convolutional neural network prediction [J]. Journal of Asian Architecture and Building Engineering, 2022, 21(3): 986-1001.

[6] GE P, HUANG W, ZHANG J R, et al. Mix proportion design method of recycled brick aggregate concrete based on aggregate skeleton theory[J]. Construction and Building Materials, 2021, 304: 124584.

[7] DAS C S, DEY T, DANDAPAT R, et al. Performance evaluation of polypropylene fibre reinforced recycled aggregate concrete[J]. Construction and Building Materials, 2018, 189: 649-659.

[8] HE W C, KONG X Q, FU Y, et al. Experimental investigation on the mechanical properties and microstructure of hybrid fiber reinforced recycled aggregate concrete [J]. Construction and Building Materials, 2020, 261: 120488.

[9] AHMED T W, ALI A A M, ZIDAN R S. Properties of high strength polypropylene fiber concrete containing recycled aggregate[J]. Construction and Building Materials, 2020, 241: 118010.

[10] CHANG H F, ZHU S J, ZHANG Z, et al. Experimental study on seismic performance of prefabricated slotted encased square steel pipe column bases[J]. Journal of Southeast University (Natural Science Edition), 2025, 55(5): 1416-1425. (in Chinese)

[11] ZHANG Y, JIANG H, WEN J, et al. A prefabricated structure scheme for thin-wall pier and seismic performance analysis[J]. 2024, 54(4): 911-920.

[12] WANG L P, WU X Y, HU M, et al. Analysis of lateral resistance performance of a novel prefabricated cold-formed thin-walled steel framed wall [J]. Journal of Southeast University (Natural Science Edition), 2024, 54(1): 135-141. (in Chinese)
[13] LUO B, WANG B, SONG Y C, et al. Study on seismic and thermal performance of prefabricated composite wall based on fiber-reinforced EPS concrete1 [J]. Journal of Southeast University (English Edition), 2025, 41(4): 501-511.
[14] LIN J R, CHEN K Y, PAN P, et al. Digital and intelligent standards for building and construction engineering: Current status and future[J]. 2025, 55(1): 16-29.
[15] ZHANG J W, LI Y D, ZHAO Y R, et al. Seismic behavior of prefabricated medium-high strength recycled concrete shear walls with high-strength steel bars in boundary elements [J]. Journal of Building Structures, 2022, 43(4): 103-113. (in Chinese)
[16] ZHANG T, HUANG W, RONG C. Damage constitutive models of polypropylene fiber recycled concrete[J]. Materials Review, 2015, 29(22): 150-155. (in Chinese)
[17] LI B, HUANG W, LI C N, et al. Study on damage constitutive model of steel fiber recycled brick aggregate concrete[J]. Journal of Huazhong University of Science and Technology (Natural Science Edition), 2017, 45(1): 17-23. (in Chinese)
[18] NING X L, DING Y N. Effect of steel fiber on the damage constitutive model of concrete under uniaxial compression [J]. Journal of Building Materials, 2015, 18(2): 214-220. (in Chinese)
[19] Ministry of Housing and Urban-Rural Development of the People's Republic of China. Standard for test method of concrete structures: GB/T 50152—2012[S]. Beijing: China Architecture and Building Press, 2012. (in Chinese)
[20] JEAN L. A continuous damage mechanics model for ductile fracture [J]. Journal of Engineering Materials and Technology, 1985, 107(1): 83-89.
[21] CAO W G, ZHAO M H, LIU C X. Study on the model and its modifying method for rock softening and damage based on weibull random distribution[J]. Chinese Journal of Rock Mechanics and Engineering, 2004, 23(19): 3226-3231. (in Chinese)
[22] GUO Z H. Principles of reinforced concrete[M]. Beijing: Tsinghua University Press, 2013. (in Chinese)
[23] JIANG J F, WU Y F, LI B B. Characteristic of internal friction angle for confined concrete[C]//Proceedings of the 23rd National Conference on Structural Engineering (Volume Ⅱ). Lanzhou, 2014:47-51. (in Chinese)
[24] CAO W G, LI X. A new discussion on damage softening statistical constitutive model for rocks and method for determining its parameters [J]. Rock and Soil Mechanics, 2008(11): 2952-2956. (in Chinese)
[25] LI L, XIAO J Z, POON C S. Dynamic compressive behavior of recycled aggregate concrete[J]. Materials and Structures, 2016, 49(11): 4451-4462.
[26] ASLANI F, HOU L J, NEJADI S, et al. Experimental analysis of fiber-reinforced recycled aggregate self-compacting concrete using waste recycled concrete aggregates, polypropylene, and steel fibers [J]. Structural Concrete, 2019, 20(5): 1670-1683.
[27] WANG J C, LI Y C, QIU Z M, et al. Experimental research on compressive properties of recycling polypropylene (PP) fiber recycled coarse aggregate concrete [J]. Journal of Building Engineering, 2023, 76: 107403.
[28] GUO Z H. Strength and deformation of concrete-experimental basis and constitutive relation [M]. Beijing: Tsinghua University Press, 1997. (in Chinese)

聚丙烯纤维再生细骨料混凝土受压损伤本构模型

罗斌, 曹广, 宋也超, 赵丰年, 唐中华

(兰州理工大学土木与水利工程学院,兰州 730050)

摘要: 为推动绿色再生类建材在建筑工程中的应用,本文基于应变等效原理与聚丙烯纤维再生细骨料混凝土(PRFAC)微元强度服从Weibull统计分布的规律,在微元破坏服从Drucker-Prager准则的条件下,建立了PRFAC的统计损伤本构模型;基于分布参数m与S_0对PRFAC本构模型曲线的分析结果,拟合出考虑细骨料取代率与分布参数的表达式,建立了以再生细骨料取代率为参数变化的统计损伤应力-应变理论曲线。结果表明,该理论曲线与实测曲线有较好的拟合度,并且能有效反映出随着再生细骨料取代率的增加,PRFAC逐渐趋向脆性等特点;此外,取代率的增加会加速PRFAC内部裂缝的发展,减弱了混凝土的变形能力和韧性,从而使得纤维再生细骨料混凝土内部的累积损伤演化过程加快。

关键词: 绿色混凝土;聚丙烯纤维;再生细骨料;损伤本构模型;受压性能;骨料取代率

中图分类号: TU375.2